THE JOURNAL OF BIOLOGICAL CHEMISTRY
Vol. 278, No. 51, Issue of December 19, pp. 50961–50969, 2003
Printed in U.S.A.


# Mammalian Mitochondrial DNA Replicates Bidirectionally from an Initiation Zone*[S]

Received for publication, July 23, 2003, and in revised form, September 5, 2003
Published, JBC Papers in Press, September 23, 2003, DOI 10.1074/jbc.M308028200

**Mark Bowmaker,[a,b] Ming Yao Yang,[a,b] Takehiro Yasukawa,[a,c] Aurelio Reyes,[a,d,e] Howard T. Jacobs,[f,g,h] Joel A. Huberman,[i,j] and Ian J. Holt[a,h,k]**

*From the [a]Dunn Human Nutrition Unit, Wellcome Trust-Medical Research Council Building, Hills Road, Cambridge CB2 2XY, United Kingdom, the [d]Sezione di Bioinformatica e Genomica di Bari, Istituto Tecnologie Biomediche, Consiglio Nazionale delle Ricerche, Via Amendola 168/5, 70126 Bari, Italy, the [f]Institute of Medical Technology and Tampere University Hospital, FIN-33014, University of Tampere, Finland and the Institute of Biomedical and Life Sciences, University of Glasgow, Glasgow G12 8QQ, United Kingdom, and the [i]Department of Cancer Genetics, Roswell Park Cancer Institute, Buffalo, New York 14263-0001*

**Previous data from our laboratory suggested that replication of mammalian mitochondrial DNA initiates exclusively at or near to the formerly designated origin of heavy strand replication, $O_H$, and proceeds unidirectionally from that locus. New results obtained using two-dimensional agarose gel electrophoresis of replication intermediates demonstrate that replication of mitochondrial DNA initiates from multiple origins across a broad zone. After fork arrest near $O_H$, replication is restricted to one direction only. The initiation zone of bidirectional replication includes the genes for cytochrome *b* and NADH dehydrogenase subunits 5 and 6.**

Neutral/neutral two-dimensional agarose gel electrophoresis (N/N 2D-AGE)[1] has been widely used to define a variety of replication intermediates (RIs) (1–4). Initiation of replication within a DNA restriction fragment gives rise to a characteristic initiation or "bubble" arc, whereas origin-less fragments that are passively replicated by forks moving from one end to the other generate characteristic "Y" arcs (5). The technique of N/N 2D-AGE has proved applicable to mapping replication origins in the whole range of living organisms, from simple plasmids (5, 6) to complex eukaryotic genomes (7, 8). The method can identify other features of the replication process such as fork arrest. Replication fork barriers (RFBs) produce spots on Y arcs (2). The higher the frequency of fork arrest, the stronger the spot and the weaker the arc downstream of the RFB.

Mitochondrial DNA of mammals is a closed circular molecule of ~16.5 kb; it encodes 13 proteins that contribute to oxidative phosphorylation (Fig. 1*A*). Replication of mtDNA has been studied in a number of organisms using N/N 2D-AGE (9–12). The patterns of RIs obtained were consistent with conventional coupled leading and lagging strand (or strand-coupled) replication. However, for many years it was believed, based initially on electron microscopic images of the mtDNA of cultured cells, that mammalian mtDNA was replicated primarily via a unique, strand-asymmetric, unidirectional mechanism (13) (Fig. 1*B*). More recently, we used N/N 2D-AGE to demonstrate that human, mouse, and rat mtDNA replication involves conventional double-stranded RIs with coupled leading and lagging strand synthesis in addition to the partially single-stranded molecules that appeared consistent with a strand-asymmetric mechanism (14). In a later study, the isolation procedure was improved, and the more highly purified mitochondria yielded only replication intermediates that were substantially duplex; moreover, the partially single-stranded forms seen in the previous study could be generated by RNase H treatment. Hence, it was concluded that mammalian mtDNA replication intermediates contain extensive ribonucleotide patches and that the apparent strand-asymmetric replication intermediates result from RNA degradation during isolation (15). Two major objections to the conclusions of this study were raised recently; the first objection is that partially single-stranded molecules (including products of strand-asymmetric replication) would not be detected by N/N 2D-AGE because of branch-migration, and the second objection is that the blocked restriction sites could arise from transcription intermediates (16). However, intact, partially single-stranded replication intermediates have been analyzed successfully using N/N 2D-AGE (17), and, in any case, branch migration of nascent DNA strands would produce a linear, single-strand arc on neutral/neutral two-dimensional agarose gels (18). Transcription intermediates would inevitably be partially single-stranded whether or not replication was occurring on the same molecule, whereas the novel, slow-moving, Y-like arcs we described were substantially duplex (15). Although extensive ribonucleotide incorporation created duplex RIs akin to strand-coupled RIs (15), it was not known where or by what mechanism these intermediates originated.

When we previously screened the mammalian mitochondrial genome for origins of replication, we detected initiation arcs exclusively in restriction fragments that included the previously defined strand-asymmetric origin of replication, $O_H$ (14). Based on this observation, we proposed that strand-coupled

* The United Kingdom Medical Research Council provided financial support for this work. The costs of publication of this article were defrayed in part by the payment of page charges. This article must therefore be hereby marked "*advertisement*" in accordance with 18 U.S.C. Section 1734 solely to indicate this fact.

[S] The on-line version of this article (available at http://www.jbc.org) contains Supplementary Data Figs. 1–4.

[b] These authors contributed equally to this study.

[c] Holder of an overseas fellowship from the Japanese Society for the Promotion of Science.

[e] Recipient of a Royal Society visiting fellowship.

[g] Supported by the Academy of Finland and Tampere University Hospital Medical Research Fund.

[h] The collaboration between these two authors is supported by European Union Project MitEURO Grant QLG1-CT-2001-00966.

[j] Supported by National Institutes of Health Grants GM49294, CA95908, and CA84302.

[k] To whom correspondence should be addressed. Tel.: 44-1223-252840; Fax: 44-1223-252845. E-mail: holt@mrc-dunn.cam.ac.uk.

[1] The abbreviations used are: NIN 2D-Age, neutral/neutral two-dimensional agarose gel electrophoresis; RI, replication intermediate; RFB, replication fork barrier; $O_H$, origin of heavy strand replication; $O_L$, origin of light strand replication; np, nucleotide pair; kbp, kilobase pair; 1n, unit length fragment.

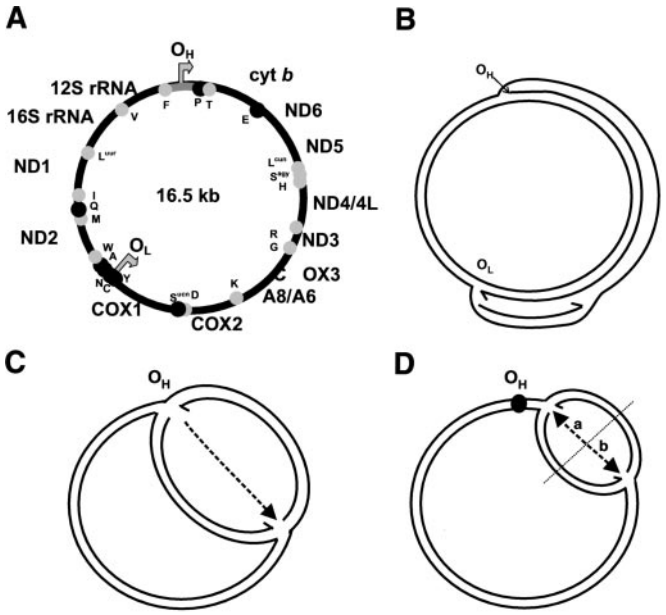


FIG. 1. **The mammalian mitochondrial genome and models of mtDNA replication.** *A*, the mammalian mitochondrial genome encodes 13 polypeptides and the RNA elements necessary for their translation. Abbreviations used on the diagram include the following: *ND*, NADH dehydrogenase; *cyt b*, cytochrome *b*; *COX*, cytochrome *c* oxidase; *A*, ATP synthase, *rRNA*, rRNA genes. The 22 transfer RNAs are denoted according to the single letter code. The $tRNA^{Pro}$ gene marks the end of the large non-coding region and the end of the D-loop. *B*, the strand asymmetric model of mammalian mtDNA replication in which both strands are synthesized continuously from physically and temporally distinct sites termed $O_H$ and $O_L$. The diagram depicts a replication intermediate where the leading strand has traversed two-thirds of the genome, exposing $O_L$ and thereby enabling second-strand synthesis to begin in the opposite direction (for details, see Ref. 13). *C*, strand-coupled unidirectional replication from a discrete origin ($O_H$) (14). $O_H$ defines both the start site for replication and the terminus; the *broken line* with an *arrowhead* indicates the direction of replication away from $O_H$. *D*, the new model supported by data presented in this report depicting bidirectional $\theta$ replication originating downstream of $O_H$ with subsequent fork arrest (fork marked *a*) at $O_H$. Note that, after the arrest of fork a, the replication intermediates associated with the different models depicted in *panels C* and *D* are indistinguishable.

replication was unidirectional, with an origin close to or coincident with $O_H$ (Fig. 1*C*). $O_H$ has been mapped precisely in humans (19) at nucleotide position (np) 191 of the 16,569 bp mtDNA molecule (20). It was mapped at np 16,008 of the (differently numbered) 16,298-bp rat mitochondrial genome (21) and at np 16,065 in the mitochondrial genome of mouse (22). However, our previous study (14) did not exclude an alternative model, namely bi-directional, strand-coupled replication, initiating at one or more sites downstream of $O_H$ and followed by fork arrest at $O_H$ (Fig. 1*D*, and Fig. 2, scenarios labeled *II* and *III*). Our original interpretation depended on the assumption that molecules derived from $O_H$-containing fragments coincident with a simple Y arc represented broken bubbles (14). The assumption was tenuous, given that it had been shown earlier that broken bubbles form arcs distinct from a simple Y arc (23).

Here we report that more detailed mapping studies refute our previous model. Instead, they support the alternative proposition in which initiation of strand-coupled ($\theta$) replication occurs downstream of $O_H$. Initiation of strand-coupled mtDNA replication is not restricted to the large non-coding region, which contains the major promoters for the two strands of mammalian mtDNA. Moreover, strand-coupled $\theta$ replication is the major mechanism of replication of mammalian mtDNA irrespective of ribonucleotide incorporation.

## EXPERIMENTAL PROCEDURES

Mitochondrial DNA was extracted from highly purified mitochondria of human placenta and mouse or rat liver as described previously (15) with one modification. Whereas mitochondria were previously lysed immediately after pelleting following isolation from a density sucrose gradient, in this study purified mitochondria were resuspended in 75 mM NaCl and 50 mM EDTA (pH 7.6) with 500 $\mu$g/ml proteinase K without detergent. After incubation at 50 °C for 30 min, mitochondria were lysed by the addition of SDS to a final concentration of 0.5%, and the incubation was extended for a further 120 min. DNA was precipitated from solution after successive phenol and chloroform extractions and resuspended in 10 mM Tris and 0.1 mM EDTA (pH 7.6). Mitochondrial DNA (0.1–1 $\mu$g) was digested with restriction endonucleases under conditions recommended by the manufacturer (New England Biolabs). Where indicated, single-strand nuclease treatment was with one unit of S1 nuclease (Promega) for 120 s at 37 °C after restriction digestion.

*Two-dimensional Agarose Gel Electrophoresis and Hybridization*—For fragments of 2–5 kilobase pairs (kbp) in size, neutral/neutral, two-dimensional agarose gel electrophoresis was performed by the standard method (3). Briefly, first dimension electrophoresis was at 0.7 V/cm for 20 h at room temperature in a 0.4% agarose gel without ethidium bromide; the second dimension gel was 1% agarose with 300 ng/ml ethidium bromide, and electrophoresis was at 6 V/cm for 4 h at 4 °C. In the case of fragments of >5 kb, first dimension electrophoresis was in a 0.35% agarose gel at 1.5 V/cm for 20 h, and second dimension electrophoresis was 3 at V/cm for 18 h in a 0.875% agarose gel. After Southern blotting, specific regions of human, mouse, or rat mtDNA were amplified by the polymerase chain reaction and then radioactively labeled using random primers. Five microliters of [$\alpha$-$^{32}$P]dCTP (3000 Ci/mmol, Amersham Biosciences) were incubated with three units of Klenow DNA polymerase and 50 ng of DNA that had been annealed with 50 ng of hexadeoxyribonucleotides for 15–30 min at 37 °C. Oligonucleotide primers and the region of mtDNA each pair amplified are listed below.

*Human mtDNA*—From Ref. 20, the oligonucleotide primers and the regions of human mtDNA they amplified were: probe h1, 5′ TAACCACTCACGGGAGCTCT-3′ and 5′-AAGGCTAGGACCAAACCTAT-3′, np 23–668; probe h2, 5′-CATGTGCCTAGACCAAGAAG-3′ and 5′-TAGAATCCGAGTATGTTGGAG-3′, np 12,499–13,922; probe h3, 5′-GAATCATCCGCTACCTTCAC-3′ and 5′-GTTTACAAGACTGGTGTATTAG-3′, np 14,977–15,926; probe h4, 5′-CTGTTCGCTTCATTCATTGC-3′ and 5′-GTCATTATGTGTTGTCGTGC-3′, np 8,540–9,212; and probe h5, 5′-AACGAATGATTTCGACTCAT-3′ and 5′-TCTGTTTGTCGTAGGCAGAT-3′ np 10,425–11,602.

*Mouse mtDNA*— From Ref. 22, the oligonucleotide primers and the regions of mouse mtDNA they amplified were: probe m1, 5′-CAAAGGTTTGGTCCTGGCCT-3′ and 5′-TGTAGCCCATTTCTTCCCA-3′, np 69–790; probe m2, 5′-CGCCTAATCAACAACCGTCT-3′ and 5′-TGGTAGCTGTTGGTGGGCTA-3′, np 8,032–8,497; probe m3, 5′-CATAGCCTGGCAGACGAACA-3′ 5′-GAGGTGGATTTTGGGATGGT-3′, np 12,777–13,435; and probe m4, 5′-CACAACCAACATCCCCCCTA-3′ and 5′-GCTGTGGCTATGACTGCGAA-3′, np 13,867–14,518.

*Rat mtDNA*— From Ref. 21, the oligonucleotide primers and the regions of human mtDNA they amplified were: probe r1, 5′-GGCATCTGGTTCTTACTTCAGGG-3′ and 5′-TGTTTTTGGGGTTTGGCATTG-3′ np 15,765–16,120; probe r2, 5′-ACCTACTAGGAGACCCAGACA-3′ and 5′-CCTGAGAAGACTGACTCTTCA-3′, np 14,866–15,331; and probe r3, 5′-GCCTACCCATTCATCATCCTCT-3′ and 5′-GTGTGGGAAGGTTGGAGGTT-3′, np 10,916–11,436. Southern hybridization was carried out in 0.25 M sodium phosphate, pH 7.2, and 7% SDS buffer overnight at 65 °C. Post-hybridization washes were 1× SSC followed by 0.1× SSC, 0.1% SDS, both for 30 min at 65 °C. Filters were exposed to x-ray film and developed after 0.5–10 days.

## RESULTS

*Initiation Arc Intensity Increases with Increasing Distance from $O_H$*—DNA fragments containing a unique unidirectional origin located toward one end, such that the incipient replication fork passes through much of the fragment, will not produce a simple Y arc. Rather, the RIs will initially contribute only a bubble arc (illustrated in Fig. 2*A*). However, AccI- and DraI-digested fragments of human and mouse mtDNA containing $O_H$ lacked an appreciable bubble arc (Fig. 3, *A* and *D*). Although bubble arcs arising from a unidirectional origin located close to the center of a fragment can be difficult to distinguish from

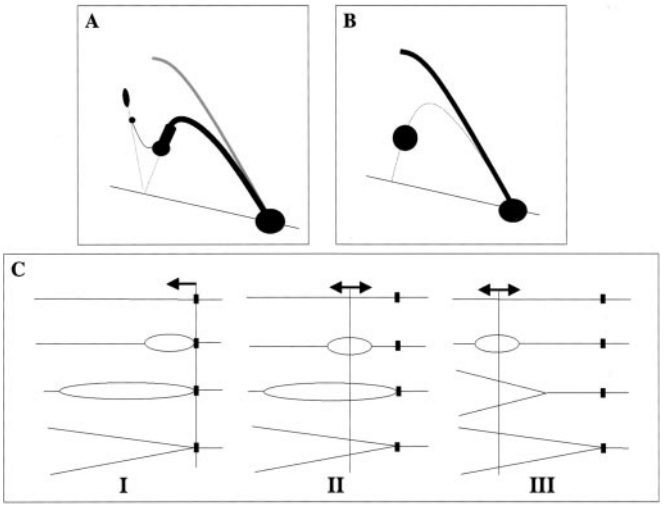


FIG. 2. **Mechanisms of initiation of mammalian mtDNA replication.** *A*, diagrammatic illustration of the previously published two-dimensional gel blot of the $O_H$-containing HincII fragment of human mtDNA (14) and Fig. 3*B*. *B*, illustration of the predicted pattern of replication intermediates (RIs) for a discrete unidirectional origin located at $O_H$. In *panel C* are three possible interpretations labeled *I*, *II*, and *III* for the scenarios discussed below. *Horizontal lines* represent linear duplex DNA molecules spanning, from left to right, np 13,637–1,008. *Vertical bars* indicate the position of $O_H$, and *arrows* show the direction(s) of replication. The previously published interpretation (14), scenario I, assumed unidirectional fork movement leftwards from $O_H$, creating a truncated bubble arc, which converts to a prominent burst bubble structure lying on the standard Y arc as the fork exits the fragment. Bidirectional initiation from one or more positions less than halfway from $O_H$ to the left-hand end of the fragment, with fork arrest at $O_H$ (scenario II), would generate exactly the same intermediates. Bidirectional initiation from one or more points further from $O_H$, with fork arrest at $O_H$ (scenario III), would generate a more truncated bubble arc plus an enhanced portion of the standard Y arc, because the leftward-moving fork would exit the fragment before the rightward-moving fork had reached $O_H$. The combination in the published gel of an enhanced portion of the standard Y arc plus an extensive bubble arc suggests that scenarios II and III, or even all three scenarios, may operate in different molecules. Scenario I cannot alone account for the pattern of RIs detected.

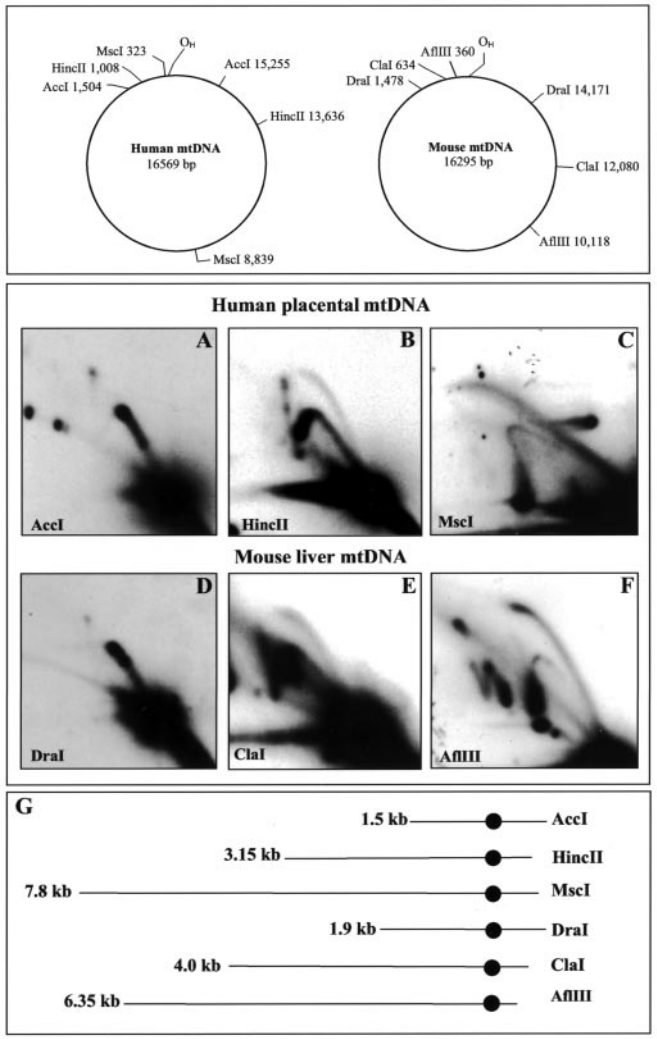


FIG. 3. **Bubble arc intensity increases with increasing distance from $O_H$.** Restriction-digested samples of human placenta mtDNA (*A–C*) and mouse liver mtDNA (*D–F*) were separated on Brewer-Fangman gels and probed for $O_H$-containing fragments of mtDNA. The restriction enzyme used appears in the *bottom left corner* of each image. Gel blots were hybridized with probe h1 (*panels A* and *B*), h2 (*panel C*), m1 (*panel D*), or m2 (*panels E* and *F*). *Panels A*, *B,* and *D* are reproduced from Ref. 14. *Panel G* shows the approximate lengths of each of the fragments analyzed aligned with respect to $O_H$ (*filled circle*). The size indicated in kilobases is the portion of the fragment downstream of $O_H$ (in the direction of the cytochrome *b* gene). A 7.3-kb BtgI fragment of mouse mtDNA spanning np 9,215–224 also yielded a prominent initiation arc similar to that associated with the 6.6-kbp AflIII fragment in *panel F* (Supplementary Data Fig. 1, available in the on-line version of this article). (For an interpretation of the image in *panel F*, see Supplementary Data Fig. 2. Another $O_H$-containing fragment lacking an appreciable bubble arc is shown in Supplementary Data Fig. 3, together with longer exposures of *panels A* and D.) Schematic maps of human and mouse mtDNA marked with restriction sites defining the probed fragments appear at the *top*.

simple Y arcs, a bubble arc was detected previously in the same fragment of mtDNA of a tumor cell line (14). Thus, the AccI result cannot be reconciled with unidirectional replication from $O_H$. Furthermore, our previous suggestion that the Y-like species resulted from bubbles broken during processing (14) is undermined by other observations. First, Hamlin and co-workers have shown that broken replication bubbles form arcs distinct from a simple Y arc (23). Second, intact bubble arcs were seen with other enzymes such as HincII and ClaI (*e.g.* Fig 3, *B* and *E*). Third, both DraI and AccI were subsequently found to yield intact bubble arcs from human or rat mtDNA when probed for fragments lacking $O_H$ (see below). Moreover, as detailed in Fig. 2, aspects of the results from the $O_H$-containing HincII fragment of human placental mtDNA, in particular the simple Y arc arising from the unit length fragment (1n), can only be reconciled with initiation of replication at one or more sites outside the fragment in some molecules. On the other hand, the weak bubble arc indicates that replication does initiate within the fragment, at least in a minority of molecules, though not necessarily at $O_H$. A slightly larger $O_H$-containing ClaI fragment of mouse mtDNA gave a similar result, *i.e.* a bubble arc accompanied by a slightly more pronounced Y arc (Fig 3*E*). The relative abundance of bubble and Y molecular species altered markedly when still larger fragments of human or mouse mtDNA were studied; the bubble arc signal increased considerably, with a concomitant decrease in signal from the simple Y arc (Fig. 3, *C* and *F*). Moreover, the absence of a detectable ascending Y arc close to 1n in the $O_H$-containing 6.6-kbp AflIII fragment of mouse mtDNA indicates that replication rarely initiates outside the fragment. Thus, both human and mouse mtDNA fragments containing $O_H$ exhibited a trend according to size; bubble arcs were barely detectable in small fragments (1.5 and 2 kbp downstream of $O_H$), moderate in intermediate sized fragments (3–4 kb downstream of $O_H$), and prominent in large fragments ($\geq$6 kb downstream of $O_H$). The quantitative differences described above were reproducible both between and within different samples; the gels shown have been selected on the basis of image quality. Therefore, these data suggest that replication initiates frequently at mul-

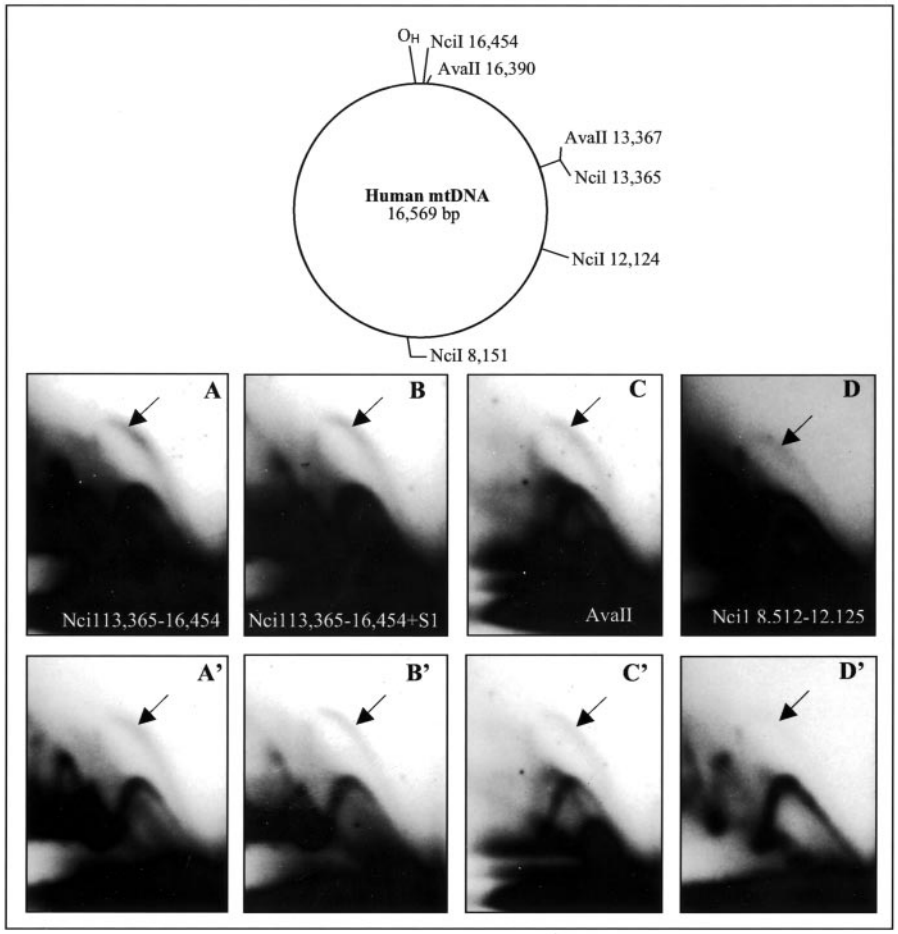


FIG. 4. **Initiation arcs associated with fragments of human mtDNA lacking $O_H$.** Mitochondrial DNA from highly purified human placental mitochondria was digested with NciI (*panels A*, *B*, and *D*) or AvaII (*panel C*). The products were separated by two-dimensional gel electrophoresis. In all cases, the detected fragment lacks $O_H$. Hence, where a bubble arc is associated with a fragment (*arrows*) it cannot be the result of unidirectional replication initiating at $O_H$ (scenario I in Fig. 2). *Panels A′–D′* are shorter exposures of *panels A–D*; these shorter exposures show that the most prominent replication intermediates form standard and slow moving Y-like arcs. Each prominent spot on the duplex linear arc greater in mass than the unit length linear fragment and the accompanying slow moving Y-like arc can be explained by ribonucleotide incorporation at the restriction site (see Ref. 21). In addition, there appeared to be a major pause site coinciding with a point on the ascending slow moving Y-like arc (*panels A′* and *C′*), which was single-strand nuclease-sensitive (*panel B′*). This species was common to all fragments of mammalian mtDNA in which one end mapped to the D-loop region (for an example, Fig. 3, C, D, and K in Ref. 21). Thus, we attribute the apparent pause to D-loop-containing molecules that were not cleaved by the restriction enzyme on the displaced strand; note, however, that this does not establish a direct relationship between D-loop-containing molecules and the molecular species forming the slow moving Y-like arc. Gel blots were hybridized with probe h3 (*panels A–C*) and probes h4 and h5 (*panel D*). A schematic map at the *top* shows the restriction sites for human mtDNA that define the fragments analyzed in *panels A–D*.

tiple sites downstream of $O_H$ and only rarely at or near $O_H$.

Two straightforward and readily testable predictions stem from these conclusions. First, initiation arcs should be detectable in fragments of mammalian mtDNA lacking $O_H$; second, the initiation arcs should not map to a single site.

*Strand-coupled Replication Initiates in Fragments of Human and Mouse mtDNA Lacking $O_H$*—Analysis of a number of mtDNA fragments lacking $O_H$, derived from purified human placenta and mouse liver mitochondria, revealed bubble arcs on neutral/neutral two-dimensional agarose gels (Figs. 4 and 5). For example, human mtDNA fragments spanning np 13,366–16,456 (NciI) and np 13,366–16,390 (AvaII) both lack $O_H$ (located at np 191); therefore, the bubble arcs associated with these fragments (Fig 4, *A–C*) must have arisen from initiation at sites other than $O_H$. In the case of the np 13,366–16,456 and np 13,366–16,390 human mtDNA fragments (Fig. 4, *A–C*), a complete Y arc was also detected, indicating that strand-coupled replication frequently initiates at sites outside the fragment. This conclusion was confirmed when the filter shown in Fig. 4*A* was reprobed for the NciI fragment spanning np 8,152–12,125, revealing a weak bubble arc (Fig. 4*D*). The disparity in signal between the bubble arcs of the two NciI fragments (np 13,366–16,456 and np 8,152–12,125) indicates that more initiation events occur in the fragment adjacent to (but not containing) $O_H$. Additional prominent non-standard arcs (slow moving Y-like arcs) were evident in many cases (*e.g.* Fig. 4, *A′–D′*); these are the result of blocked restriction enzyme sites attributable to extensive ribonucleotide incorporation on the newly synthesized mitochondrial L-strand (for details, see Ref. 15).

A number of fragments of mouse mtDNA lacking $O_H$ analyzed by N/N 2D-AGE also revealed a complete bubble arc and a complete Y arc, such as an NsiI fragment spanning np 10,758–15,903 (Fig. 5*A*) and a BglI fragment spanning np 12,664–15,949 (Fig. 5*B*). Bubble arcs were also detected in a XbaI fragment (np10,907–15,973), a PsiI fragment (np 10,971–15,590), and a BanII fragment (np 12,959–15,742), which similarly lack $O_H$ (data not shown). A unidirectional origin located close to the common end of these various fragments, around np 15,500, with synthesis away from $O_H$, could explain these data. However, a complete bubble arc was also detected associated with an AccI fragment of mouse mtDNA spanning np 9,599–

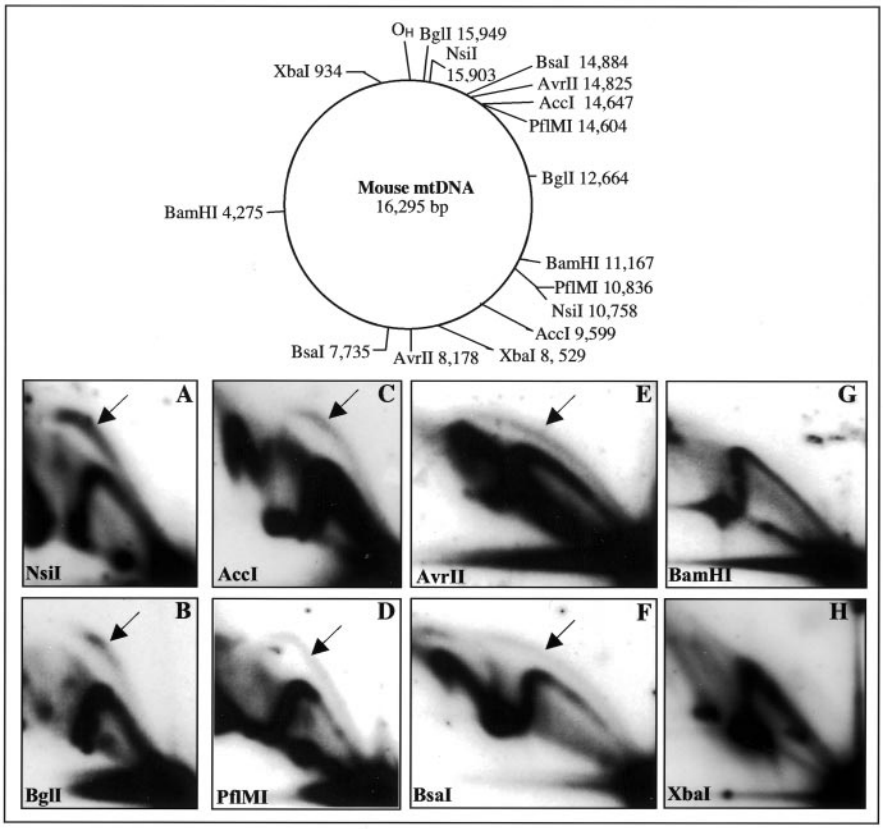


FIG. 5. **Initiation arcs are associated with overlapping fragments of mouse mtDNA lacking $O_H$.** Purified mouse liver mtDNA samples were digested with NsiI (*panel A*), BglI (*panel B*), AccI (*panel C*), PflMI (*panel D*), AvrII (*panel E*), BsaI (*panel F*), BamHI (*panel G*), or XbaI (*panel H*). Gel blots were hybridized with probe m2 (*panels A* and *B*), m3 (*panels C–F*), or m4 (*panel G*). Each detected fragment lacks $O_H$. A schematic map at the *top* shows the restriction sites for mouse mtDNA that define the fragments analyzed in *panels A–G*.

14,647 (Fig 5*C*) and a PflMI fragment spanning np 10,836–14,604 (Fig. 5*D*). Thus, if unidirectional replication is to account for these findings, there must be a third origin close to the ends of these fragments around np 14,500, with the direction of synthesis again away from $O_H$. Alternatively, bi-directional replication initiates at multiple sites downstream of $O_H$, with one advancing fork undergoing arrest upon reaching $O_H$. Consistent with the latter interpretation is the pronounced thickening of the descending portion of the Y arc in several fragments, most notably as seen in Fig. 5*D*. Moreover, multiple unidirectional origins of similar strength cannot account for the abrupt termination of the Y arc in $O_H$-containing fragments, which indicates that many replication intermediates share a common end mapping at or near $O_H$. Although $O_H$ acting as the major unidirectional origin would be compatible with this observation, the absence of bubble arcs in some $O_H$-containing fragments (Fig 3, *A* and *D*) and their weakness in others (Fig. 3, *B* and *E*) categorically contradict this idea. Therefore, only bidirectional replication from multiple origins with the subsequent arrest of one advancing fork at $O_H$ is compatible with all the data (Fig. 2*C*, scenarios labeled *II* and *III*).

Analysis of larger fragments of mouse mtDNA, such as a 6.65-kbp AvrII fragment (np 8,178–14,825) (Fig. 5*E*) and a 7.15 kbp BsaI fragment (np 7,735–14,884) (Fig. 5*F*), yielded a similar ratio of bubble to simple Y molecules as smaller fragments, such as the AccI fragment spanning np 9,599–14,647 (Fig. 5*C*). This suggests that the first fork to exit the fragment does so at the $O_H$ proximal end (14,825, 14,884, or 14,647). Only large fragments containing $O_H$ produced a prominent bubble arc; therefore, the majority of bubbles of 5 kb or more include a fork that has reached and stalled at $O_H$. As mentioned above, the $O_H$-containing AflII fragment of mouse mtDNA lacked a portion of the ascending Y arc close to 1n, suggesting that few origins are located in the 2 kb of the fragment furthest from $O_H$ (circa np 10,118–12,000). Further evidence that origins are not scattered throughout the mouse mitochondrial genome came from a 6.9 kb BamHI fragment (np 4,275–11,167) and a 7.6kb XbaI fragment (np 938–8,529), each of which lacked a bubble arc and was associated with a simple Y arc (Fig 5, *G* and *H*, respectively). Other fragments of mammalian mtDNA that lacked an initiation arc are described below.

*Replication Origins of Rat mtDNA Map to a Broad Region Downstream of $O_H$*—Analysis of mtDNA replication intermediates in rat liver lends support to the idea that bidirectional initiation in a zone downstream of $O_H$ is general among mammalian mtDNAs. As with human and mouse mtDNA, bubble arc *versus* Y arc intensity was greater in large fragments containing $O_H$ than small $O_H$-containing fragments (Fig. 6, *A versus B* and *C*). The presence of a prominent simple Y arc arising from 1n in the small fragments (Fig. 6, *B* and *C*) again suggests that initiation events occur not only downstream of $O_H$ but also outside these fragments, *i.e.* at nucleotide numbers below 13,811. Moreover, given that the bubble arc was more truncated than the Y arc in such fragments, unidirectional $\theta$ replication initiating at $O_H$ is excluded as a major mode of replication for rat liver mitochondria. Unidirectional replication from $O_H$ would produce a bubble arc that extended to a point in line with the terminus of the bubble arc (marked with a *vertical broken line* in Fig. 6*C*). The smear on the descending Y arc that ends abruptly in a pronounced spot (Fig. 6*D*) suggests that replication fork arrest occurs at multiple loci. Therefore, the data in rat are consistent with the initiation of bidirectional replication in the $O_H$-distal portion of the restriction fragment (np ~14,500–15,000), followed by stalling of the rightward-moving replication fork within a ~500-bp region terminating at $O_H$. Alternative initiation events further from $O_H$ within this fragment, or outside the fragment altogether, could account for the prominent Y arc signal. The replication forks coming from these more $O_H$-distal origins would also stall

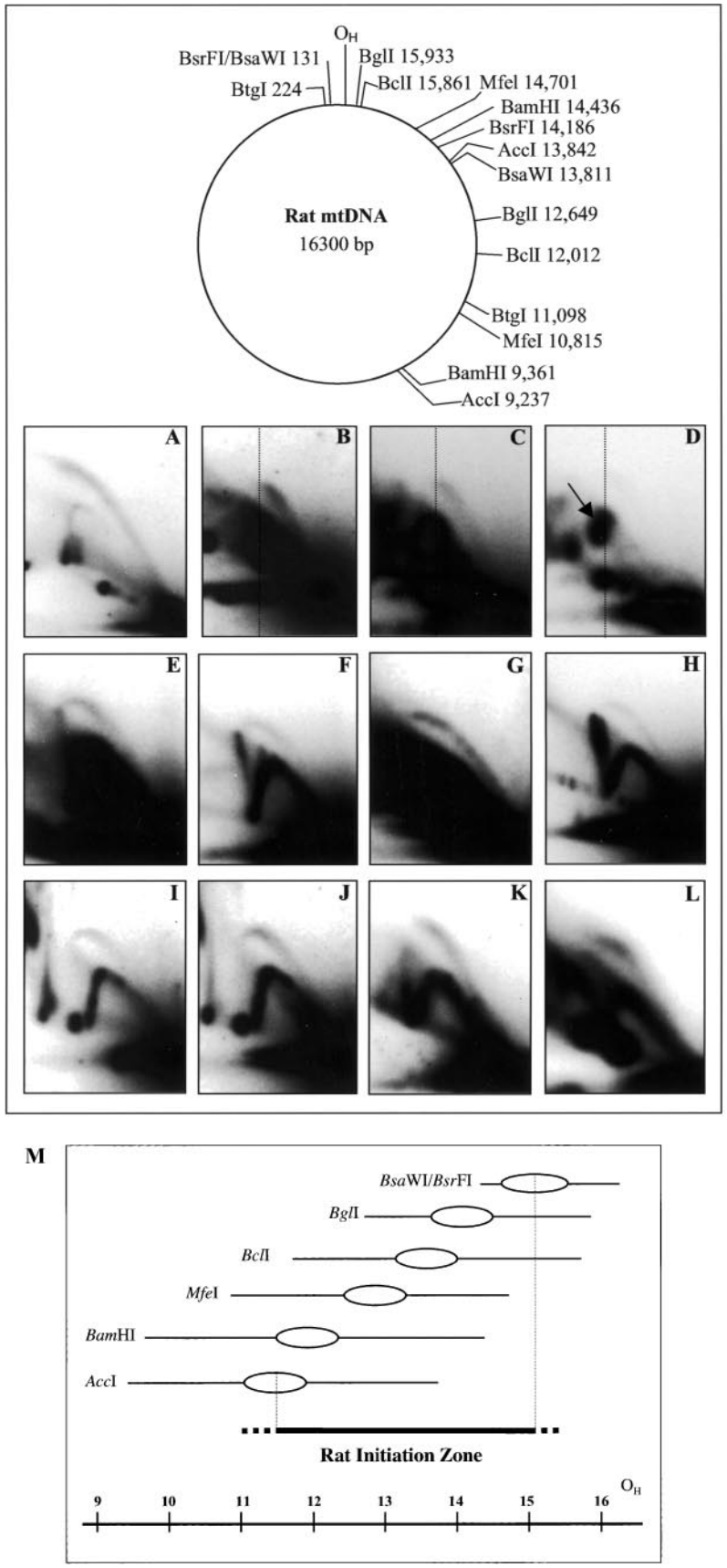


FIG. 6. **A series of overlapping fragments of rat mtDNA is associated with initiation arcs.** A schematic map at the *top* indicates the restriction sites defining the fragments of rat mtDNA that were associated with an initiation arc. Rat liver mtDNA was digested with BtgI (*panel A*), BsaWI (*panel B*), BsrFI (*panels C* and *D*), AccI (*panels E* and *F*), MfeI (*panels G* and *H*), BamHI (*panels I* and *J*), BglI (*panel K*), or BclI (*panel L*) and then treated (*panels F*, *H*, and *J*) or not treated (*all other panels*) with S1 nuclease prior to two-dimensional electrophoresis. S1-resistant molecules cannot be the products of either strand-asymmetric replication or transcription that entails extensive RNA-DNA hybrid formation, as both of these processes would generate partially single-stranded molecular forms. Gel blots were hybridized with probe r1 (*panels C* and *D*), r2 (*panels A*, *B*, *K*, and *L*), or r3 (*panels E–J*). The initiation arcs are more truncated than the Y arcs in *panels B* and *C* and are marked by a *broken vertical line*. *Panel D* is a shorter exposure of *panel C*; the *arrow* in *panel D* indicates a portion of the Y arc that forms a prominent smear, which is consistent with replication pausing in a region that terminates at or near $O_H$. Note that the BclI site at 13,389 (21) was absent in all rat mtDNA samples analyzed. Two other fragments of rat mtDNA, a DraI fragment (np 13,177–15,516) and an NdeI fragment (np 12,741–15,633) yielded complete or nearly complete bubble arcs, whereas an HgaI fragment (np 12,217–211) revealed a truncated bubble arc (data not shown). Prominent X-like spikes were evident in some digests (*panels F* and *H*); typically, these are characteristic of recombination intermediates. Such forms appear with high abundance in all fragments of human heart mtDNA (46), although their role in mtDNA homeostasis is an enigma. *Panel M*, the initiation zone of bidirectional strand-coupled replication of rat mtDNA**.** Fragments of rat mtDNA that produced a bubble arc are aligned with a portion of the rat mitochondrial genome; a set of overlapping restriction fragments were each associated with a complete bubble arc, yet the fragments do not share a common end or mid-point. The only model compatible with the data is one in which bidirectional replication initiates heterogeneously within the zone indicated in different molecules.

near $O_H$ and would contribute to the strength of the pause region signal on the Y arc.

To test for the possibility of alternative initiation events $O_H$-distal to 14,500, we examined other restriction fragments of rat mtDNA. Analysis of the 4.6-kb AccI fragment (np 9,236–13,841), the MfeI fragment (np 10.815–14,701), and the BamHI fragment (np 9,361–14,436) all yielded bubble arcs (Fig 6, *E–J*). Bgll and Bcll fragments of rat mtDNA adjacent to, yet lacking,

$O_H$ and mapping between np 12,643 and np 15,927 were also associated with bubble arcs (Fig. 6, *K* and *L*). These data support the view that rat mtDNA replication is initiated by a strand-coupled $\theta$ mechanism at multiple sites downstream of $O_H$.

*Fine Mapping of the Origin of Strand-coupled Replication in Rat mtDNA*—Analysis of overlapping fragments of DNA has been used previously to map origins of replication, (*e.g.* Ref. 24). A complete bubble arc is consistent with bidirectional replication from an origin located at the center of a fragment; in practice, an origin anywhere within the central third of a fragment (sometimes called the "detection zone") gives rise to a clear bubble arc, whereas origins closer to the ends of fragments are difficult, if not impossible, to detect by N/N 2D-AGE (25). Where replication is unidirectional, only origins at the extreme end of a fragment will produce a complete bubble arc. Accordingly, overlapping fragments on either side of a fragment in which such an origin is located will, in one case, lack the origin, whereas in the other case the pattern formed will be a truncated bubble arc accompanied by a double Y arc. None of these scenarios is consistent with the results. In the case of rat mtDNA, the AccI (np 9,237–13,842), BamHI (np 9,361–14,436), BglI (np 12,643–15,927), and BclI (np 12,012–15,861) fragments cover a region that overlaps the extreme fragments (AccI and BglI) by less than half their length, yet all were associated with essentially complete bubble arcs (Fig. 6, *D–J*). A discrete origin, whether bidirectional or unidirectional, would give alterations in the patterns of bubble-, Y-, and X-shaped replication intermediates when overlapping fragments were compared.

The only explanation consistent with the data is that bidirectional $\theta$ replication initiates at different positions in different molecules and that these origins are scattered throughout an extensive zone stretching approximately from 500 base pairs downstream of $O_H$ (in the rat) to the ND4 gene. Based on this analysis, $\theta$ replication initiates in a zone that spans approximately np 11,500–15,500 of rat mtDNA (Fig. 6*M*). The data sets for mouse and human indicate mtDNA initiation zones of np 11,300–15,500 and np 10,500–16,000, respectively. Discrete origins, such as the SV40 origin, give rise to bubble arcs that are particularly prominent near their apex (26). The prominent apex of the bubble arc of mouse mtDNA (Fig. 3*F*) contrasts with that of human (Fig. 3*C*) and is consistent with a narrower initiation zone in mouse than human mtDNA. In any event, the exact boundaries of the initiation zone may be slightly outside of the defined limits, because origins of $\theta$ replication located near one end of a fragment are difficult to detect (25). Conversely, the breadth of the zone may be exaggerated by the absence of informative sites. Where two forks of a bidirectional origin travel at different speeds, the size of the zone would be exaggerated in the direction of the slower moving fork. Origins do not need to be evenly dispersed across an initiation zone, nor do all origins need to be activated at equal frequency. In human mtDNA, $\theta$ replication appears to be more frequent in the $O_H$ proximal part of the initiation zone. There are a number of reports of initiation zones, including several in mammalian nuclear DNA such as, for example, dihydrofolate reductase (27), $\beta$-globin (28), and immunoglobulin H loci (29).

*Absence of Coupled Replication Origins in Other Regions of Mammalian mtDNA*—The above data indicate that mammalian mtDNA origins are dispersed across a wide zone in three different species, namely rat, mouse, and human. However, this zone does not encompass the entire genome, much of which is free of origins that give rise to initiation arcs on N/N 2D-AGE. The fragments that define a contiguous origin-free zone covering the rest of the mitochondrial genome are as follows: in rat, np 15,861–2,340, 7,654–12,012, 2,340–7,654, 3,066–6,204, and 16,183–3,066; in human, 3,659–7,658 and 1,505–6,259; and in mouse, 16,174–2,349, 934–8,529, 3,102–7,084, 4,275–11,167, 5,276–9,817, 7,084–11,322, and 14,647–5,710 (see Supplementary Data Fig. 4 in the on-line version of this article).

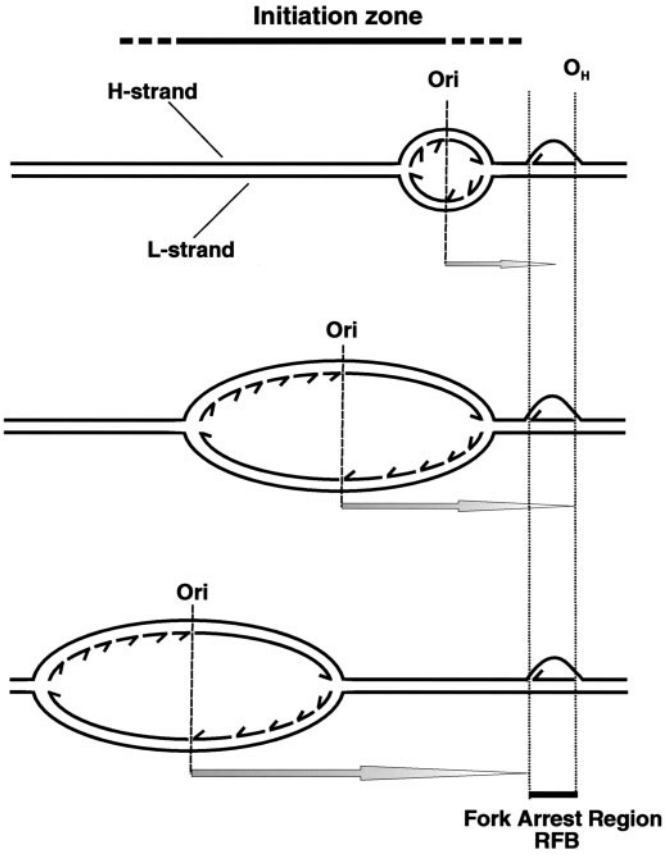


FIG. 7. **Proposed model of bi-directional initiation of replication of mammalian mitochondrial DNA.** Replication initiation is depicted originating at multiple sites (*Ori*) that lie in a defined region (see "Discussion" for details); replication is bi-directional, however, a directional RFB maps to a position in the major non-coding region close to the locus designated previously as the origin of heavy (leading) strand synthesis. The $O_H$ proximal fork stalls at or within ~500 bp of $O_H$. The model is based on the observations in this report. Origins of replication map to the center of different, partially overlapping fragments of mammalian mtDNA, indicating that initiation occurs at multiple sites; origins are dispersed over a region of 4–6 kbp, and one end of the initiation zone maps to within a kilobase of the 3′ end of the D-loop. Replication forks rarely pass through the entire fragment where it contains $O_H$, which suggests that forks frequently stall in this region. Stalling may be mediated by short D-loops whose 5′-ends map to $O_H$. Replication fork arrest predominates at a locus, which maps within 200 bp of $O_H$; nevertheless, some forks arrest downstream of $O_H$ within the region defined by the short D-loop, suggesting that triple-stranded (or triplex) DNA may precipitate replication fork arrest, albeit at a relatively low frequency compared with $O_H$.

## DISCUSSION

N/N 2D-AGE has been employed widely since 1987 and is the pre-eminent method for analyzing replication intermediates, including origins of replication (1, 30, 31); to date, it has proved to be totally reliable. In the present study, extensive analysis of mitochondrial DNA of three mammals revealed a set of overlapping fragments associated with initiation arcs (Figs. 3–6). These data are indicative of multiple origins of replication distributed across a region of four or more kilobases located downstream of the 3′-end of the short displacement loop.

*Can the Initiation Arcs Account for All the Observed mtDNA Replication Intermediates?*—Many of the initiation arcs derived from mammalian mtDNA were relatively weak compared

with the accompanying standard Y arcs (Figs. 4–6). The question therefore arises as to whether replication might sometimes initiate elsewhere, but by another mechanism that does not generate a standard bubble arc on two-dimensional gels. Where bidirectional replication initiates at multiple sites, most initiation events will occur toward one end or the other of a restriction fragment; hence, one replication fork will exit the fragment before the other, the bubble structure will be cleaved by the restriction enzyme, and a partial Y arc will be created (Supplementary Data Fig. 5, available in the on-line version of this article.). Any initiation event outside the fragment will contribute a complete Y arc. Thus, a zone of initiation predicts a prominent standard replication fork (Y) arc to accompany the initiation arc. This is exactly what was seen for the well characterized dihydrofolate reductase (DHFR) locus of nuclear DNA (24, 27). Replication fork arrest will, of course, prevent one fork from exiting a fragment; thus, the increased prominence of initiation arcs in large $O_H$-containing fragments is entirely consistent with our model for mtDNA that proposes a bi-directional initiation zone downstream of a powerful RFB ($O_H$). Because the majority of RIs of human, mouse and rat mtDNA form classical bubble arcs in large $O_H$-containing fragments (Fig. 3, *C* and *F*, and Fig. 6*A*), we conclude that strand-coupled $\theta$ replication arising from multiple origins is the major mechanism of replication for mammalian mtDNA, at least for the tissues examined. Furthermore, because the large $O_H$-containing fragments studied here include sites that are known to be ribonucleotide blocked, *e.g.* at nps 13,842 and 14,632 of rat mtDNA (15), the simple and slow-moving Y arcs described previously (15) must be generated by a common ($\theta$) mechanism. Otherwise molecules comprising the initiation arc would form a minority of replication intermediates associated with large $O_H$-containing fragments, which was not the case (Fig 3, *C* and *F*, and Fig 6*A*).

*Unidirectional versus Bidirectional Replication—Escherichia coli* plasmids such as Col E1 were long-believed to replicate in a unidirectional manner, and this mechanism appeared to be confirmed by N/N 2D-AGE analysis (6). However, a later, more detailed study of a closely related plasmid (p15A) indicated that replication is initially bidirectional (32), as proposed here for mammalian mitochondrial DNA. Fork direction analysis of mtDNA fragments would add support to the model because it predicts that, for fragments outside the initiation zone, replication forks will enter at the end proximal to the 3′-end of the D-loop.

*Role of $O_H$ and the D-loop in mtDNA Replication*—In our revised model, $O_H$ acts not as the origin of strand-coupled replication but as a terminus for mtDNA replication. $O_H$ is always preserved in partially deleted mtDNAs, whereas most, if not the entire, initiation zone of human mtDNA as defined in this report is redundant (33). Similarly, in the most extensively studied replication initiation zone, the human nuclear dihydrofolate reductase locus, all sequence elements are known to be dispensable (34). The most obvious candidate for an essential *cis*-element for mtDNA replication outside the initiation zone is the triple-stranded D-loop region, located in the major non-coding region (35, 36). Short regions of triplex DNA are known to inhibit transcription (for an example, see Ref. 37); hence, the function of the D-loop may be to mediate replication fork arrest by forming a structural barrier. An attractive feature of this hypothesis is that it can account for the observed stalling, not at a single site, but across a region of several hundred base pairs (*e.g.* Fig. 3, *A* and *D*, and Fig. 6*D*). The fact that replication almost never extends upstream of $O_H$ toward the ribosomal DNA genes suggests that any fork reaching $O_H$ stalls at that point. By analogy with *E. coli* Col E1 (38), this could be due to the inability of the replisome helicase to separate regions of RNA-DNA hybrid formed by the short D-strand primer and which persist in mtDNA after replication. If D-loops do indeed mediate fork arrest of $O_H$-proximal replication forks (Fig. 7), then the vast majority of replicating molecules must have arisen from molecules containing a D-loop, as almost all of them appear to undergo fork arrest in the D-loop region. Therefore, either D-loop synthesis is so frequent that there is generally a D-loop present in each molecule that initiates replication or, more likely, the D-loop itself provides the conditions under which replication can initiate in the zone downstream of it via topological alteration of mtDNA structure. In this regard, it is noteworthy that regions of triplex DNA can promote homologous recombination at sites up to 4 kb distant (39). In our revised model, $O_H$ serves as a bidirectional replication terminus. It should be noted that the predicted "double Y" arcs associated with replication termination are often very faint or not discernible above the background of the strong stall at $O_H$. Double Y arcs in $O_H$-containing fragments are more clearly detectable in mtDNA from cultured cells recovering from induced mtDNA depletion, although they are not seen under standard growth conditions (see Fig. 7 of Ref. 14). This suggests that the final stages of mtDNA replication are completed rapidly under normal conditions.

*Mitochondrial DNA Replication and Pathological Rearrangements*—Pathological rearrangements of human mtDNA invariably spare $O_H$ and the D-loop, whereas the region that contains the initiation zone is frequently deleted (33, 40, 41). As well as indicating the functional importance of $O_H$, this also suggests that the zone itself does not supply the signals essential for initiation of replication. Perhaps any DNA located downstream of the D-loop could function as an origin zone because of its proximity to the D-loop and membrane components (42). Indeed, this may be a general feature of initiation zones; as mentioned above, the signals essential for nuclear dihydrofolate reductase gene replication have recently been shown to lie outside the well characterized initiation zone (34).

Another feature of pathological rearrangements of human mtDNA is that they commonly occur in the major arc between $O_H$ and $O_L$ (40, 41). Replication fork arrest is a well recognized prelude to genome rearrangement (43–45). An RFB is located close to $O_L$ (14), and the data reported here suggest that $O_H$ acts as a prominent RFB. Taken together, these observations offer a partial explanation for the location of pathological rearrangements; that is, molecules in which replication has stalled at the fork barriers near $O_H$ and $O_L$ may be favored substrates for illicit recombination.

*Acknowledgments*—We thank Jen Chi-Min and Joanna Poulton, University of Oxford, for helpful discussions on the possible role of the D-loop in mitochondrial DNA replication. We also thank Lodovica Vergani, University of Padova, for help in preparing human mitochondrial DNA samples.

REFERENCES

1. Brewer, B. J., and Fangman, W. L. (1991) *BioEssays* **13,** 317–322
2. Brewer, B. J., and Fangman, W. L. (1988) *Cell* **55,** 637–643
3. Friedman, K. L., and Brewer, B. J. (1995) *Methods Enzymol.* **262,** 613–627
4. Wang, S., Dijkwel, P. A., and Hamlin, J. L. (1998) *Proc. Natl. Acad. Sci. U. S. A.* **95,** 14757–14762
5. Brewer, B. J., and Fangman, W. L. (1987) *Cell* **51,** 463–471
6. Martin-Parras, L., Hernandez, P., Martinez-Robles, M. L., and Schvartzman, J. B. (1991) *J. Mol. Biol.* **220,** 843–853
7. Dijkwel, P. A., Vaughn, J. P., and Hamlin, J. L. (1992) *Chromosoma* **102,** S17–S23
8. van Brabant, A. J., Hunt, S. Y., Fangman, W. L., and Brewer, B. J. (1998) *Electrophoresis* **19,** 1239–1246
9. Han, Z., and Stachow, C. (1994) *Chromosoma* **103,** 162–170
10. Lockshon, D., Zweifel, S. G., Freeman-Cook, L. L., Lorimer, H. E., Brewer, B. J., and Fangman, W. L. (1995) *Cell* **81,** 947–955
11. Mayhook, A. G., Rinaldi, A. M., and Jacobs, H. T. (1992) *Proc. R. Soc. Lond. B Biol. Sci.* **248,** 85–94
12. Preiser, P. R., Wilson, R. J., Moore, P. W., McCready, S., Hajibagheri, M. A.,

Blight, K. J., Strath, M., and Williamson, D. H. (1996) *EMBO J.* **15,** 684–693
13. Clayton, D. A. (1982) *Cell* **28,** 693–705
14. Holt, I. J., Lorimer, H. E., and Jacobs, H. T. (2000) *Cell* **100,** 515–524
15. Yang, M. Y., Bowmaker, M., Reyes, A., Vergani, L., Angeli, P., Gringeri, E., Jacobs, H. T., and Holt, I. J. (2002) *Cell* **111,** 495–505
16. Bogenhagen, D. F., and Clayton, D. A. (2003) *Trends Biochem. Sci.* **28,** 357–360
17. Belanger, K. G., Mirzayan, C., Kreuzer, H. E., Alberts, B. M., and Kreuzer, K. N. (1996) *Nucleic Acids Res.* **24,** 2166–2175
18. Holt, I. J., and T., J. H. (2003) *Trends Biochem. Sci.* **28,** 355–356
19. Crews, S., Ojala, D., Posakony, J., Nishiguchi, J., and Attardi, G. (1979) *Nature* **277,** 192–198
20. Anderson, S., Bankier, A. T., Barrell, B. G., de Bruijn, M. H., Coulson, A. R., Drouin, J., Eperon, I. C., Nierlich, D. P., Roe, B. A., Sanger, F., Schreier, P. H., Smith, A. J., Staden, R., and Young, I. G. (1981) *Nature* **290,** 457–465
21. Gadaleta, G., Pepe, G., De Candia, G., Quagliariello, C., Sbisa, E., and Saccone, C. (1989) *J. Mol. Evol.* **28,** 497–516
22. Bibb, M. J., Van Etten, R. A., Wright, C. T., Walberg, M. W., and Clayton, D. A. (1981) *Cell* **26,** 167–180
23. Kalejta, R. F., Lin, H. B., Dijkwel, P. A., and Hamlin, J. L. (1996) *Mol. Cell. Biol.* **16,** 4923–4931
24. Dijkwel, P. A., and Hamlin, J. L. (1999) *Methods* **18,** 418–431
25. Linskens, M. H., and Huberman, J. A. (1990) *Nucleic Acids Res.* **18,** 647–652
26. Kalejta, R. F., and Hamlin, J. L. (1996) *Mol. Cell Biol.* **16,** 4915–4922
27. Vaughn, J. P., Dijkwel, P. A., and Hamlin, J. L. (1990) *Cell* **61,** 1075–1087
28. Aladjem, M. I., Rodewald, L. W., Lin, C. M., Bowman, S., Cimbora, D. M., Brody, L. L., Epner, E. M., Groudine, M., and Wahl, G. M. (2002) *Mol. Cell. Biol.* **22,** 442–452
29. Zhou, J., Ashouian, N., Delepine, M., Matsuda, F., Chevillard, C., Riblet, R., Schildkraut, C. L., and Birshtein, B. K. (2002) *Proc. Natl. Acad. Sci. U. S. A.* **99,** 13693–13698
30. Raghuraman, M. K., Brewer, B. J., and Fangman, W. L. (1994) *Genes Dev.* **8,** 554–562
31. Dijkwel, P. A., Vaughn, J. P., and Hamlin, J. L. (1994) *Nucleic Acids Res.* **22,** 4989–4996
32. Kuzminov, A., Schabtach, E., and Stahl, F. W. (1997) *J. Mol. Biol.* **268,** 1–7
33. Mita, S., Rizzuto, R., Moraes, C. T., Shanske, S., Arnaudo, E., Fabrizi, G. M., Koga, Y., DiMauro, S., and Schon, E. A. (1990) *Nucleic Acids Res.* **18,** 561–567
34. Mesner, L. D., Li, X., Dijkwel, P. A., and Hamlin, J. L. (2003) *Mol. Cell. Biol.* **23,** 804–814
35. Gillum, A. M., and Clayton, D. A. (1978) *Proc. Natl. Acad. Sci. U. S. A.* **75,** 735–739
36. Kasamatsu, H., Robberson, D. L., and Vinograd, J. (1971) *Proc. Natl. Acad. Sci. U. S. A.* **68,** 2252–2257
37. Ritchie, S., Boyd, F. M., Wong, J., and Bonham, K. (2000) *J. Biol. Chem.* **275,** 847–854
38. Santamaria, D., de la Cueva, G., Martinez-Robles, M. L., Krimer, D. B., Hernandez, P., and Schvartzman, J. B. (1998) *J. Biol. Chem.* **273,** 33386–33396
39. Biet, E., Sun, J. S., and Dutreix, M. (2003) *Nucleic Acids Res.* **31,** 1006–1012
40. Moraes, C. T., DiMauro, S., Zeviani, M., Lombes, A., Shanske, S., Miranda, A. F., Schon, E. A., Nakase, H., Bonilla, E., Werneck, L. C., Servidei, S., Nonaka, I., Koga, Y., Spiro, A. J., Brownell, K. W., Schmidt, B., Schotland, D. L., Zupanc, M., DeVivo, D. C., and Rowland, L. P. (1989) *N. Engl. J. Med.* **320,** 1293–1299
41. Holt, I. J., Harding, A. E., Cooper, J. M., Schapira, A. H., Toscano, A., Clark, J. B., and Morgan-Hughes, J. A. (1989) *Ann. Neurol.* **26,** 699–708
42. Albring, M., Griffith, J., and Attardi, G. (1977) *Proc. Natl. Acad. Sci. U. S. A.* **74,** 1348–1352
43. Rothstein, R., Michel, B., and Gangloff, S. (2000) *Genes Dev.* **14,** 1–10
44. Hyrien, O. (2000) *Biochimie (Paris)* **82,** 5–17
45. Bidnenko, V., Ehrlich, S. D., and Michel, B. (2002) *EMBO J.* **21,** 3898–3907
46. Kajander, O. A., Karhunen, P. J., Holt, I. J., and Jacobs, H. T. (2001) *EMBO Rep.* **2,** 1007–1012